Chinese Journal of Physics 67 (2020) 376–387

Contents lists available at ScienceDirect

Chinese Journal of Physics

journal homepage: www.elsevier.com/locate/cjph

Features of superconducting transition in nanocomposite consisting of "insulating matrix (porous alkali-borosilicate glass)" – "granular metallic filler (indium)"

O.N. Ivanov[a,b,*], A.V. Fokin[c], Yu.A. Kumzerov[c], A.A. Naberezhnov[c]

[a] Belgorod State University, Belgorod, 308015, Russian Federation
[b] Belgorod State Technological University named after V.G. Shukhov, Belgorod, 308012, Russian Federation
[c] Ioffe Institute, St. Petersburg, 194021, Russian Federation

ARTICLE INFO

Keywords:
Nanocomposite
Porous glass
Granular conductor systems
Superconducting transition
Fluctuation conductivity

ABSTRACT

Patterns in temperature and magnetic field behavior of the electrical resistance of nanocomposite consisting of "insulating matrix (7 nm-pore alkali-borosilicate glass)" – "granular metallic filler (indium)" (PG7 + In) has been found and analyzed in the vicinity of superconducting transition. Insulating behavior in the electrical resistivity has been observed in a normal state. External magnetic field shifts the transition to lower temperatures and the same time gradually strengths the insulating behavior above the superconducting transition. Hopping conductivity mechanism developed for the granular conductor systems can be responsible for the insulating behavior in normal-state electrical resistance. Electron hopping in the granular conductor system is realized as tunneling of electrons through intergranular contacts between the metallic granules. The superconducting transition has been found to be rather broad. Broadening in the superconducting transition can be attributed to fluctuation conductivity. Above the superconducting transition, the Aslamazov-Larkin contribution to the conductivity characteristic for three-dimensional systems has been found to be main correction to the conductivity.

1. Introduction

Any granular conductor system consists of close-packed metallic granules possessing a high enough conductivity, separated by intergranular insulating boundaries [1]. If sizes of the conducting granules are corresponding to nanometer scale, these granular conductor systems should be considered as a new class of artificial nanomaterials. The physical properties of individual nanocrystals and coupled nanocrystals can be combined in the granular conductor systems. Depending on intergranular coupling strength, the granular conductor system can behave itself either as a metal or as an insulator. Therefore, the intergranular coupling strength is the fundamental and often the tuned parameter, governing the electrical properties of granular conductor systems. A few of technological methods can be applied to prepare the granular conductor systems with controlled and varying intergranular coupling strength. Traditional methods are thermal evaporation and sputtering techniques [2,3]. Modern methods include self-assembled methods focusing on preparation of colloidal nanocrystals [4,5] and epitaxial growth methods of two semiconductors with significantly different lattice constants, which are used to prepare semiconductor quantum dot arrays [6,7]. One more prospective approach to construct the granular conductor systems is fabrication of nanocomposites consisting of metallic nanosized granules embedded into

* Corresponding author.
E-mail address: Ivanov.Oleg@bsu.edu.ru (O.N. Ivanov).

https://doi.org/10.1016/j.cjph.2020.07.003
Received 27 March 2020; Received in revised form 28 June 2020; Accepted 7 July 2020
Available online 23 July 2020

the pores of insulating nanoporous glass matrix [8–10]. Shape and size of pores, and arrangement and dimensionality of porous structure determine the basic parameters of this granular system, including granule size, a ratio between volumes of insulating and conducting subsystems, dimensionality of conducting subsystem, pores filling factor et cet. All these parameters affect on the intergranular coupling strength.

Among various types of filler material, there has been much interest in superconducting metals like Hg, Pb, Ga, Sn and In [11–16]. Owing to size effects, the superconductors with characteristic sizes in nanometer range demonstrate often the specific anomalies of physical properties such as: (i) remarkable enhancing of superconducting transition temperature, (ii) crossover from the type-I superconductor behavior to the type-II one at application of magnetic field, (iii) developing a fluctuation conductivity at the superconducting transition and so on. Above the superconducting transition (i.e. in the normal state), bulk metal superconductors listed above behave themselves like normal metals, i.e. their electrical resistance R(T) gradually decreasing on cooling down to transition in the superconducting state. In contrast to the bulk analogues, the dependence R(T) for nanocomposites with the same metals embedded into the pores of nanoporous glass can transformed from the usual metallic behavior to the insulating one. If coupling between the granules is sufficiently strong, the granular system becomes well conducting. In case of low coupling the granular system behaves itself as an insulator. In the last case, superconducting transition takes place from a normal state, which is characterized by an insulating behavior of electrical resistivity, i.e. the resistivity is gradually increasing on cooling. Possible modification of R(T) from metallic type to insulating one above the superconducting transition temperature is one more important feature distinguishing the granular conductor/superconductor systems from their bulk analogues. By changing intergranular coupling from strong to weak one, the various granular conductor systems undergoing the superconductor transition from either metallic or insulating normal state can be prepared.

The aim of this paper is to find and analyze the features in temperature and magnetic field behavior of the electrical resistance in the superconducting nanocomposite consisting of “nanoporous glass matrix” – “granular indium filler”.

2. Materials and methods

Porous alkali-borosilicate glass used as matrix for nanocomposite preparation was prepared by leaching a sodium borosilicate glass. After leaching, the porous glass was cleaned by H_2O. To remove H_2O, the glass was dried at 400 K in air atmosphere during 4–6 h. The porous glass consisted of SiO_2 matrix with grid of mutually crossing disordered channels with diameter of ~7 nm (PG7). Liquid indium was embedded into the porous glass matrix under high pressure of 9 Kbar at temperature of 440 K. After solidification, indium served as a filler in the nanocomposite PG7 + In. Details of the nanocomposite fabrication are presented in Ref. [11].

Scanning electron microscope (Nova NanoSEM 450) using an energy dispersive X-ray spectroscopy (EDX) method was applied to characterize the nanocomposite. To measure the electrical resistance, R, rectangular bar samples with dimensions of $2 \times 2 \times 6$ mm^3 were prepared. Opposite faces of the bar perpendicular to its long side were covered by silver paste. Voltage drop across these faces was measured. The resistance was measured by using Mini Cryogen Free Measurements System (Cryogenic Ltd, UK) at direct current of 0.1 mA by averaging voltage values applied for forward and reverse current directions. External magnetic field, B, oriented perpendicularly to the current direction could be also applied to the sample at the R measurements.

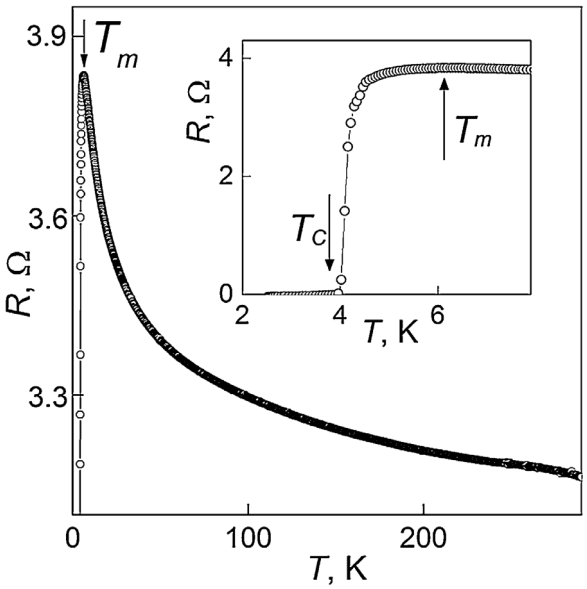

Fig. 1. The *R(T)* dependence at zero magnetic field. On inset: the *R* vs. *T* dependence in the vicinity of T_m in enlarged scale.

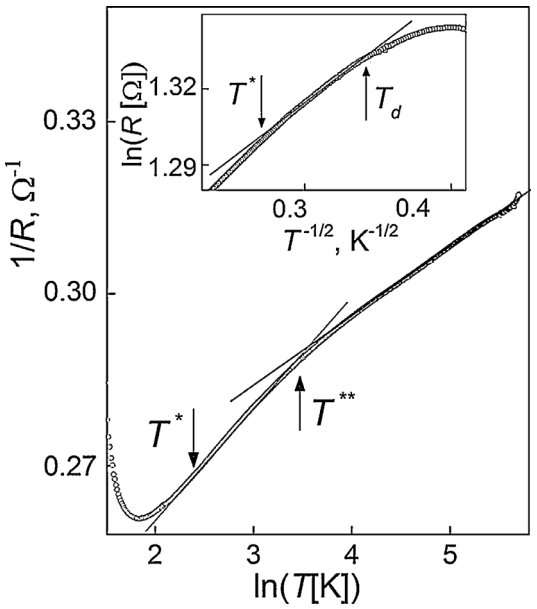

Fig. 2. The $1/R$ vs. ln$T$ dependence at zero magnetic field. On inset: the ln$R$ vs. $T^{-1/2}$ dependence at zero magnetic field.

3. Results and discussion

The $R(T)$ dependence for the nanocomposite in the temperature range $2 \div 290$ K at zero magnetic field is shown in Fig. 1. Starting from 290 K, R increases steadily on cooling down to the temperature T_m equal to 6.40 K. This $R(T)$ dependence is typical for insulators (semiconductors), but not for metals. Below T_m the growth of R is suddenly changed to falling of resistance. The $R(T)$ falling is related to transition from high-temperature normal state with $R \neq 0$ into low-temperature superconducting state with $R = 0$ (inset in Fig. 1). For bulk indium, the $R(T)$ dependence within normal state is metallic type, i.e. the resistance is gradually decreasing on cooling down to the superconducting transition [17].

Before analysing the superconductor transition in the nanocomposite, let us consider briefly the insulating $R(T)$ behavior. It is known that in the granular conductor systems, temperature behavior the conductivity (σ) at not very low temperatures can be often described by logarithmic dependence as follows [1]

$$\sigma(T) = a + b\ln T, \tag{1}$$

where a and b are the constants depending on substances.

The logarithmic temperature dependence of σ have been observed in disordered systems as well as systems with reduced dimensions. For all systems weak localization or electron–electron interaction effects have been found in the papers [2, 18-21]. Currently, the exact origins resulting in the logarithmic dependence of σ are still being debated [21]. In accordance with expression (1), the $R(T)$ dependence shown in Fig. 1 can be replotted as the $1/R$ vs. T dependence Fig. 2). Two linear segments crossing at the temperature $T^{**} \approx 35$ K can be easily found in this dependence. High-temperature segment is positioned from T^{**} up to 290 K, whereas low-temperature segment covers the interval from T^{**} down to $T^* \approx 12$ K. Hence, expression ((1) can be really applied to describe the insulating $R(T)$ behavior within T^* - 290 K interval. The a and b parameters in expression (1) will be different for the high-temperature and low-temperature linear segments. Here, we will not discuss the mechanisms responsible for the insulating $R(T)$ behavior observed above T^*. We will focus on the insulating $R(T)$ behavior observed below T^*, that is in vicinity of the superconducting transition. It is worth mentioning at this point that below T^* and down to temperature T_d, the ln(R) vs. $T^{-1/2}$ dependence is linear one (inset in Fig. 2). T_d is equal to ~9 K for zero magnetic field and very strongly dependent on magnetic field. These features will be discussed in detail below.

Inset in Fig. 1 demonstrates the $R(T)$ behavior observed in the vicinity of T_m. Although R starts to fall just below T_m, zero value of the resistance, corresponding to completing of superconducting transition, is reaching at lower temperature T_{c0} equal to 3.90 K. Temperature of the superconducting transition, T_{cb}, in bulk pure indium is known to be equal to 3.41 K, what is remarkably lower than $T_{c0} = 3.90$ K observed for the nanocomposite. That is, T_c for indium in the nanoporous alkali-borosilicate glass is enhanced over T_{cb} for bulk pure indium by ~14%. The T_{c0} value extracted for the nanocomposite is in satisfactory agreement with results reported in Refs. [13–15]. This enhancing of the superconducting transition temperature can be related to the large surface-to-volume ratio characteristic for metallic granules, which are distributed inside nanopores of the glass matrix. In turn, this large ratio can result in enhancing in the electron-phonon coupling constant through softening phonon mode. For spherical granules having average radius r, the enhancement factor (T_{c0}/T_{cb}) can be expressed as [22]

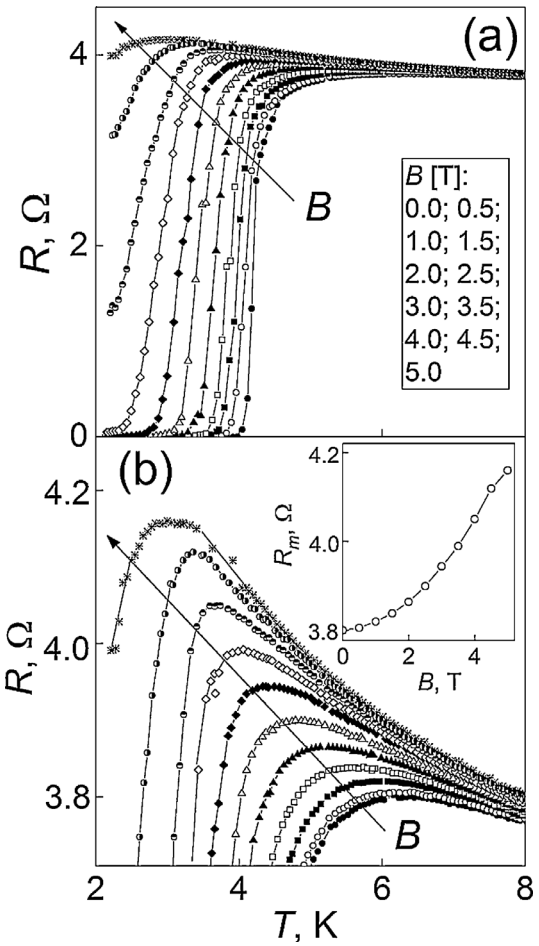

Fig. 3. (a) Magnetic field effect on the superconducting transition; (b) The R vs. T dependences in the vicinity of T_m at various values of magnetic field. Inset: the R_m vs. B dependence.

$$\frac{T_{c0}}{T_{cb}} = \frac{1}{1 + 0.674(a_0/r)} \times exp\left[\frac{1.04(1+\lambda^b)}{\lambda^b - 0.1(1+\lambda^b)} - \frac{1.04(1+k\lambda^b)}{k\lambda^b - 0.1(1+0.63k\lambda^b)}\right], k = \frac{1 + 0.674(a_0/r)}{1 - 0.551(a_0/r)}, \quad (2)$$

where a_0 is the interatomic distance and λ^b is the electron-phonon coupling constant for the bulk metal.

For bulk indium, a_0 and λ^b are known to be 3.3 Å and 0.71, respectively [22]. If average diameter of the pores (~7 nm) is taken as r, then by using expression (2), the enhancement factor can be estimated as ~1.2. This theoretical estimate is in satisfactory agreement with the experimental T_{c0}/T_{cb} value. Difference between the experimental value and the theoretical estimate can be attributed to deviation in real shape of the granules from spherical one. Superconducting transition in many conventional metals is rather narrow with transition width equal to ~0.1 K [23]. To characterize the width of the superconducting transition in the nanocomposite, the $\Delta T_{mc} = T_m - T_{c0}$ value can be introduced. This value is equal to ~2.5 K for the $R(T)$ curve, presented on inset in Fig. 1. Thus, the superconducting transition is rather broad. Broadening in the superconducting transition is one of specific features of the granular superconductors. This feature can be originated from fluctuation conductivity that effects on the $R(T)$ dependence in the granular system [1,11,24,25]. Analysis of the $R(T)$ dependence, taking into account the fluctuation conductivity corrections, will be presented below.

At the next stage, the strong magnetic field effect on the superconducting transition has been found and studied. Transverse magnetic fields with B = 0.0; 0.5; 1.0; 1.5; 2.0; 2.5; 3.0; 3.5; 4.0; 4.5 and 5.0 T have been applied at these $R(T)$ measurements. The superconducting transition was found to be shifted to lower temperatures under magnetic fields applied (Fig. 3(a)). To show the B-effect on R more detailed, the highest temperature in this Figure is limited by 8 K. For $B \leq 3$ T, the superconducting transition is totally completed, i.e. superconducting state with $R = 0$ can be yielded in the temperature range studied, and, hence, the T_{c0} values for different magnetic fields can be also extracted. For $B > 3$ T, the electrical resistance also starts to fall at T_m, but and at lowest temperature of 2 K the resistance is yet retaining non-zero value. Hence, for these B the superconducting transition is incomplete yet, and the T_{c0} temperature cannot be measured. Bulk indium is known to be the type-I superconductor with critical magnetic field equal to 0.0125 T at 2.5 K [12]. So critical magnetic field for the nanocomposite happened is much higher as compared to that for bulk indium.

As it has been reported earlier [13,15], indium in the porous glass under external magnetic field behaves as type-II superconductor. For type-II superconductors, superconducting state starts to be destroyed at lower critical field (B_{cl}) but complete suppressing superconductivity takes place only at upper critical magnetic field (B_{cu}). Between B_{cl} and B_{cu}, superconducting and normal phases coexist, but the volume ratio between these phases is changed with varying B. To explain the enhanced critical field of the nanocomposite, some features of the granular conductor systems should be taken into account. At and below B_{cl} the individual indium granules in the porous glass become superconducting, whereas at and below B_{cu}, all the superconducting granules are already coupled [15]. Granules size in the nanoporous glass matrix is limited by pore size [26]. Relevant decreasing in electron mean free path will reduce coherence length (ξ) in the granules as compared to that for bulk superconducting metal. Upper critical magnetic field is related to ξ by expression

$$B_{cu} = \frac{\phi_o}{2\pi} \times [\xi(T)]^{-2}, \tag{3}$$

where Φ_0 is the magnetic flux quantum.

In accordance with expression (3), B_{cu} should be really increasing with decreasing ξ. The R_m value corresponding to T_m has been found to be remarkably increasing with increasing B. This tendency is confirmed by the data, presented in Fig. 3(b). The $R(T)$ maximum related to the superconducting transition becomes more and more expressed at gradual increasing in magnetic field. The $R_m(B)$ dependence is shown in inset to Fig. 3(b). Magnetic field, shifting the superconducting transition to lower temperatures, at the same time broads the temperature range of the insulating $R(T)$ behavior, spreading it to the lower temperatures. In other words, magnetic field, supressing the superconducting transition, recovers the low-temperature $R(T)$ dependence, characteristic for normal/insulating state that has been before masked by transition itself. The insulating $R(T)$ behavior, observed in the nanocomposite PG7 + In, is qualitatively different from the $R(T)$ behavior, characteristic for bulk indium (metallic behavior). This difference can originated from forming granular structure of indium, embedded into the pores of the glass matrix. The granular conductor systems are electrically inhomogeneous and disordered systems, consisting of metallic granules with high enough electrical conductivity, distributed inside the insulating matrix. In accordance with Refs. [11,26], the nanocomposite can be considered as a bundle of single mutually crossing In nanowires in the glass making up a three-dimensional grid of nanowires with cells with ~20 nm size and nanowire diameters of ~7 nm. Since pores filling factor is usually less than 100%, metallic filler cannot form a continuous media. In this case, each of In nanowires can also consist of numerous granules that can be separated or clustered into extended enough islands. Actually, in accordance with the data of Ref. [27], indium in the porous glass can really form nanosized clusters. “Diffraction” sizes of these clusters estimated from broadening in the Bragg peaks in X-ray pattern is equal to ~15 nm (along the nanowires) and ~11 nm (across the nanowires). Hence, the In granules are slightly elongated along the nanowires. According to the EDX analysis, the nanocomposite is characterized by elemental composition as follows: 52.04 at.% (O), 37. 40 at.% (Si) and 10.56 at.% (In). For this elemental composition, the weight ratio of the elements is 26.90 wt.% (O), 33.94 wt.% (Si) and 39.16 wt.% (In). Then, pores filling factor can be estimated as ~65%.

One of fundamental quantum size effects, specific for the granular conductor systems at low temperatures, is pronounced discreteness of electronic levels due to electron confinement within an individual granule [1]. The mean level spacing (δ) in the granule can be determined as $\delta = (\nu \bullet V)^{-1}$, where V is the granule volume and ν is the density of states at the Fermi energy. Thus, δ is inversely proportional to V. If granule size is corresponding to several nanometers, then δ is equal to several Kelvin degrees. For example, δ is ~1 K for aluminum granule having radius $r = 5$ nm. One can conclude that the discreteness of the electronic levels can be neglected to analyze the $R(T)$ behavior in the nanocomposite studied. Then, hopping transport of electrons based on their tunneling through potential barriers, related to the granular structure, can be considered as main conductivity mechanism, responsible for the insulating $R(T)$ behavior. Generally, the intergranular electron coupling can be related to tunneling process. It is known [1], that key parameter affecting on the most of the physical properties of the granular conductor systems is an average tunneling conductance, G, between neighboring granules. In turn, this quantity is related to dimensionless intergranular (tunneling) conductance, g, measured in units of the quantum conductance, $e^2/\hbar$, i.e. $g = G/(2e^2/\hbar)$, where e is the elementary charge and $\hbar$ is the Planck's constant. The granular systems with $g \geq 1$ are characterizing by metallic transport behavior, while those with $g \leq 1$ are usually behaving as insulators. Besides, g is usually assumed to be much smaller than the intragranular conductance g_o. Usually, the intragranular conductance is due to electron scattering on impurities or granule boundaries. For strong intergranular coupling in the granular system, the electrons move easily from one to another granule under external electric field. But, for weak intergranular coupling, the insulating state is already forming due to strong Coulomb correlations that block electron transport at low temperatures. Besides the Coulomb interaction effects, the quantum interference resulting in localization of electron states at absence of interaction should be also taken into account for low conducting granular systems. Naturally, at high enough temperatures and for metallic regime of the conductivity, both Coulomb correlation and interference effects in the granular conductor systems will be weak enough. It should also be noted that the intergranular electron coupling strength will strongly effect on forming superconducting state in the granular conductor systems. Since the coupling reduces phase fluctuations, the systems with strongly coupled granules will be able to maintain superconducting coherence in whole sample. But, in case of weak coupling, strong Coulomb interaction can result in the Coulomb blockade of the Cooper pairs. Long-range superconducting order in the granular conductor system is known to take place when the Josephson coupling between neighboring granules exceeds the Coulomb charging energy [1,28,29]. Indeed, the Josephson coupling tends to lock the phases of the granules and delocalize the Cooper pairs, while the Coulomb interaction tends to localize the Cooper pairs and, hence, enhance the quantum phase fluctuations. Comparing the Josephson energy, J, with the Coulomb energy, E_c, one can conclude that the granular conductor systems with $g > g_s \sim E_c/\Delta$ (Δ is the superconducting energy gap) are superconducting systems, while those with $g < g_s$ are insulating systems. Estimation of ability of some granular conductor system,

being transformed into long-range superconducting state based on comparing E_c and J, is known as the Anderson-Abeles criterion. The criterion predicts that superconductivity may take place even in such granular systems that behave as insulators, if they have been made from normal granules under equivalent conditions. Indeed, in accordance with Ref. [1], for the granular conductor systems with the small ratio of $E_c/\Delta << 1$, there is a parametrically large interval of the conductance, $E_c/\Delta << g << 1$, where superconductivity should exist, although corresponding normal material would be insulator. Actually, granular samples of some conductor systems show really the clear insulating behavior above temperature of the superconducting transition, confirming this prediction [30, 31].

The insulating $R(T)$ behavior in the PG7 + In nanocomposite is really expressed very weakly. Actually, in accordance with the data presented in Fig. 3(b), the $\Delta R(T)/R(8\ \mathrm{K}) = [R_m - R(8\ \mathrm{K})]/[R(8\ \mathrm{K})]$ is changed from ~0.9% at $B = 0$ T to ~9% at $B = 5$ T. It means that at zero magnetic field the electrical properties of the nanocomposite is very close to a boundary, which distinguishes metallic behavior ($g \geq 1$) and insulating behavior ($g \leq 1$). That is, the g conductance can be believed to be close to unit and, hence, one can conclude that $G \approx 2e^2/\hbar$. At gradual increasing of magnetic field, the insulating behavior becomes more expressed, that is obviously related to gradual decreasing in G, but the $R(T)$ change corresponding to the insulating behavior is still remained small enough. So the insulating $R(T)$ behavior of the nanocomposite is rather corresponding to so-called weak insulator [1].

The conductivity in the granular materials in insulating state can be often described as hopping conductivity in the same manner as in heavily doped and disordered semiconductors [1, 32]

$$\sigma \sim exp\left[-\left(\frac{T_0}{T}\right)\right]^{1/2}, \tag{4}$$

where T_0 is a characteristic temperature depending on the particular microscopic characteristics.

For heavily doped and disordered semiconductors, this expression is corresponding to variable-range hopping (VRH) conductivity of the Shklovskii–Efros type [27]. In these solids, hopping conductivity starts to be developing as electron gets ability to tunnel from one to another localized state within some energy band, related to either impurity or structural disorder. There are the nearest neighbor hopping conductivity (NNH) and VRH conductivity. At NNH conductivity, the electron localized in initial state obtains energy sufficient to hop to the nearest localized state. Thermal energy of the electrons will limit the hopping conductivity in this case. Probability of the electron thermal activation between states, which are close in space but far in energy, is gradually decreasing on cooling. At some temperature, this probability becomes smaller than probability of electron hopping between some more remote states whose energy levels are very close to each other. Therefore, the transition to VRH conductivity will take place. Average hopping distance in VRH conductivity is steady increasing at temperature decreasing. The hopping conductivity is one of the main mechanisms of low temperature conductivity, applying to describe features in the electrical properties of many heavily doped and disordered semiconductors [33–39].

The model of the granular conductor system, resulting in expression (4), considers this system as an array of the identical in size and shape, but mesoscopically different metallic particles, and the intergranular electron coupling is described via a tunneling matrix [1]. To analyze both metallic and insulating behaviors of conductivity, the granule arrangements can be taken either periodic or irregular. For the insulating behavior, an electrostatic disorder in the granular system can be taken into account via random potential, V_i (i is the granule index). This potential results in a flat bare density of states at the Fermi level. In turn, this potential is induced by carrier traps in insulating matrix of the granular conductors. In this case the traps with energies lower, than the Fermi level, are charged and induce the potential of e^2/kr order on the closest granule (k is the dielectric constant of the insulator and r is the distance from the granule to the trap). This potential is comparable with the Coulomb blockade energies, resulted from charging metallic granules during the transport process. The random potential V_i, applied to each granule, will lift the Coulomb blockade on part of the granules. Then the conductivity will be mediated by electron hopping between the sites, where the Coulomb blockade is practically lifted. The electron hopping in the granular conductor system can be realized as tunneling via virtual electron levels in a sequence of the granules. The virtual electron tunneling through a single granule can be attributed to two different mechanisms of a charge transport in the Coulomb blockade regime. At the first of them known as elastic co-tunneling, the charge is transferred via the tunneling of the electron through an intermediate virtual state in the granule. In this case, energy of the electron is constant during the tunneling process. In the second mechanism of inelastic co-tunneling, energy of the electron coming out the granule is different from energy of the electron incoming in the granule. To absorb the in- and out- energy differences, the electrons leaves behind in the granule the electron-hole excitation. It should be noted that both elastic co-tunneling and inelastic co-tunneling are realized via classically inaccessible intermediate states, i.e. both mechanisms take place in form of the charge transfer via virtual states. Elastic co-tunneling is the dominant mechanism for the hopping conductivity at low temperatures, while inelastic co-tunneling processes take place at higher temperatures. Tunneling probability is falling off exponentially with increasing distance. This behavior coincides with exponentially decaying probability of tunneling between the localized states near the Fermi level in the theory of Mott-Efros-Shklovskii, developed for heavily doped and disordered semiconductors [27]. Thus, the hopping processes in both semiconductors and granular conductors systems are implemented in the same manner and, hence, can be described by the same expression (4).

Let us to apply the expression (4) to analyze the $R(T)$ dependences for the nanocomposite PG7 + In. These dependences taken for the temperature $T^* = 12\ \mathrm{K} \div T_m$ ranges and for different values of B have been replotted for the $\ln R - T^{-1/2}$ coordinates Fig. 4). For convenience, the data in this Fig. are shifted along vertical axis by using $\Delta R = 0.05\ \Omega \bullet m$, where $m = 0, 1, 2, 3, 4, 5, 6, 7, 8, 10$, and 11 for $B = 0.0$; 0.5; 1.0; 1.5; 2.0; 2.5; 3.0; 3.5; 4.0; 4.5 and 5.0 T, respectively. As it was mentioned above (inset in Fig. 2), the $\ln R = f(T^{-1/2})$ dependences can be divided on the two parts separated by some temperature T_d. Below T_d these dependences are very close to the fitting lines (dashed lines in Fig. 4). Hence, they correspond to expression ((4), but above T_d the experimental curves start to

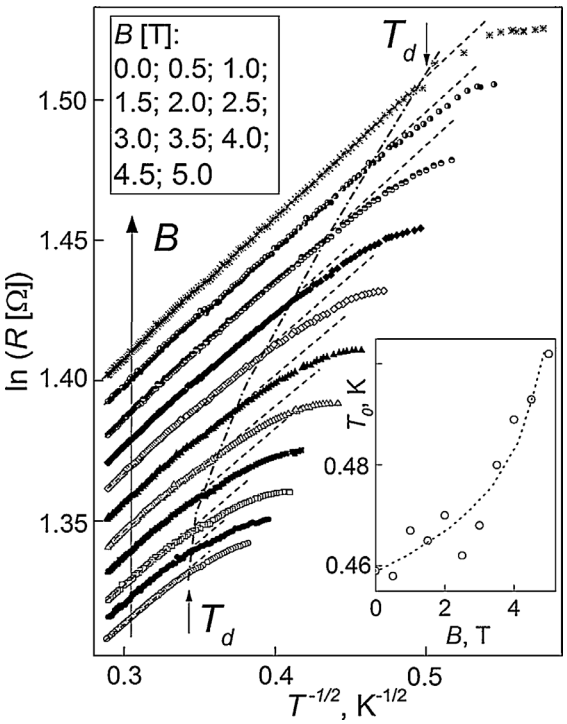

Fig. 4. The ln$R$ vs. $T^{-1/2}$ dependences at various magnetic fields. The T_d corresponds to the temperature above which the experimental dependence starts to deviate from the fitting line. Dash-dotted line allows to trace the change of T_d at varying B. Inset: the T_0 vs. B dependence.

deviate from the fitting lines. Since T_d is shifted to lower temperatures with increasing B, the temperature $T^* \approx 12$ K ÷ T_d range also increases simultaneously, i.e. the temperature range, corresponding to the hopping conductivity, is gradually broaden under magnetic field. This effect obviously connects with supressing the superconducting transition by external magnetic field. Dash-dotted line in Fig. 4 allows tracing in the T_d change at B increasing. The slope of the fitting lines in Fig. 4 can be used for estimation of the T_0 values. These values have been found to be very weakly B-dependent, as shown in the inset in Fig. 4. Since the temperature range, used to take the $R(T)$ dependences, is rather corresponding to low temperatures, let us believe that co-tunneling mechanism is responsible for the hopping conductivity in this case. For co-tunneling mechanism, the T_0 temperature can be expressed as

$$T_0 \sim \frac{e^2}{a\tilde{k}\xi_l}, \tag{5}$$

where a is the average granule size, $\tilde{k}$ is the effective dielectric constant and ξ_l is the dimensionless localization length. In turn, the tunneling probability, P_{el}, is dependent on ξ_l in accordance with expression

$$P_{el} \sim exp\left(-\frac{2s}{\xi_l}\right), \tag{6}$$

where s is the distance along the tunneling path.

It is obviously, that under magnetic field applied both ξ_l and P_{el} are slightly decreasing with increasing B. It should be noted that at the hopping conductivity the decreasing of localization length is usually connected to shrinkage of electron wave functions in a direction perpendicular to B [29]. It should be noted that now one more temperature (T_d), besides T_m and T_{c0}, can also be used to characterize the B-effect on the superconducting transition. The $T_m(B)$, $T_{c0}(B)$ and $T_d(B)$ dependences are presented in Fig. 5(a).

As it was mentioned above, the T_{c0} temperature could be measured only for $B \leq 3$ T. Since magnetic field supresses a superconductivity gradually shifting the superconducting transition to the lower temperatures, all of these temperatures are naturally decreased with increasing B. Like the temperature interval ΔT_{mc} introduced above, the temperature interval $\Delta T_{dc} = T_d - T_{c0}$ can be also used to estimate the width of the superconducting transition. In addition, another interval $\Delta T_{dm} = T_d - T_m$ would be usefully included also to analyze the $R(T)$ behavior. The magnetic field dependences of ΔT_{dc}, ΔT_{mc} and ΔT_{dm} are presented in Fig. 5(b). Again, the $\Delta T_{dc}(B)$ and $\Delta T_{mc}(B)$ dependences have been extracted for $B \leq 3$ T. For these magnetic fields, all of three dependences presented in Fig. 5(b) are weakly B-dependent. For $B > 3$ T, ΔT_{dm} decreases rapidly with increasing B.

Thus, above T_d and up to 12 K, the $R(T)$ dependences taken at various magnetic fields Fig. 4) are satisfactory obeyed the expression ((4), extracted from the tunneling conductivity mechanism in the granular conductor systems. Then, the fitting ln$R$ vs. $T^{-1/2}$ line prolonged below T_d can be considered as background change in the total $R(T)$ behavior due to the superconducting transition. This background change should be taken into account to extract the correct $R(T)$ behavior, originated from the

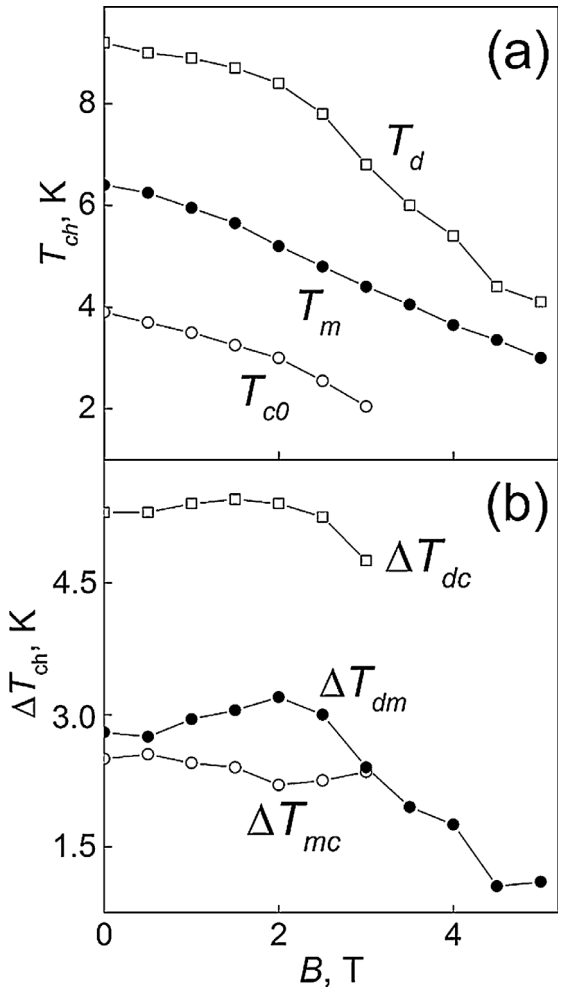

Fig. 5. (a) The magnetic field dependences of the T_d, T_m and T_c temperatures; (b) The magnetic field dependences of the temperature intervals $\Delta T_{dc} = T_d - T_{c0}$, $\Delta T_{dm} = T_d - T_m$ and $\Delta T_{mc} = T_m - T_{c0}$.

superconducting transition. To do so, the background change have to been subtracted from the experimental $R(T)$ curve to get the $\Delta \ln R(T) = \ln R(T) - \ln R_b(T)$ values. Finally, relative change in R, corresponding to the $[\Delta R(T) = R(T) - R_b(T)]/R(T)$ values, can be recovered within the ΔT_{dc} interval. Naturally, $\Delta R(T)/R(T)$ is equal to 0 (totally normal state) for $T \geq T_d$, and equal to 1 (totally superconducting state) for $T \leq T_{c0}$. If the electrical resistance in the nanocomposite is believed to be directly connected to change in ratio between the volumes of normal and superconducting states during the superconducting transition, then gradual change in $\Delta R(T)/R(T)$ from 0 to 1 will be corresponded to growth in the volume fraction of the superconducting transformed state, V_{sp}, on cooling. In other words, the $\Delta R(T)/R(T)$ ratio can be believed to be $V_{sp}(T)$.The $V_{sp}(T)$ dependences taken at various magnetic fields are shown in Fig. 6.

Under the $V_{sp} = 0.5$ condition, the fractions of normal and superconducting phases are equal. The T_c temperature corresponding to this condition can be taken as temperature of the superconducting transition midpoint. The $T_c(B)$ dependence for $B \leq 3$ T is shown in the inset in Fig. 6. The T_c temperature can be now used to characterize asymmetry in the superconducting transition. To do so, the magnetic field dependences of the $\Delta T_{HT} = T_d - T_c$ and $\Delta T_{LT} = T_c - T_{c0}$ temperature intervals have been plotted (Fig. 7(a)). First of these intervals characterizes obviously a width of the superconducting transition for high-temperature side above T_c, while ΔT_{LT} corresponds to low-temperature side. For totally symmetric superconducting transition, the ΔT_{HT} and ΔT_{LT} values should be equal to each other. Since ΔT_{HT} is far larger than ΔT_{LT} for all B values (i.e. high-temperature side of the superconducting transition in the nanocomposite is broader as compared to its low-temperature side), this transition should be considered as sufficiently asymmetric one. Moreover, with increasing magnetic field, ΔT_{HT} decreases gradually, whereas ΔT_{LT} increases little by little. So, at application of magnetic field, the superconducting transition becomes more symmetric. To underline this tendency, some asymmetry coefficients can be introduced as $\Delta T_{HT}/\Delta T_{dc}$ and $\Delta T_{LT}/\Delta T_{dc}$, where $\Delta T_{dc} = T_d - T_{c0}$ is obviously taken as total width of the superconducting transition. The magnetic field dependences of the $\Delta T_{HT}/\Delta T_{dc}$ and $\Delta T_{LT}/\Delta T_{dc}$ coefficients are shown in Fig. 7(b). In this case, totally symmetric superconducting transition will take place under clear condition of $\Delta T_{HT}/\Delta T_{dc} = \Delta T_{LT}/\Delta T_{dc} = 0.5$. Value of these coefficients equal to 0.5 is shown by dashed line in Fig. 7(b). For all magnetic fields, the $\Delta T_{HT}/\Delta T_{dc}$ values happens to be more 0.5,

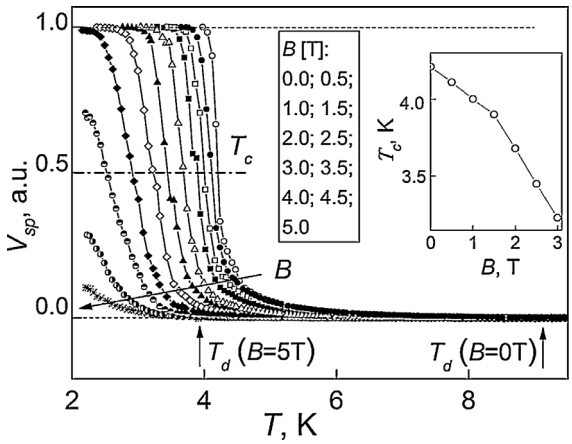

Fig. 6. The V_{sp} vs. T dependences at various magnetic fields. The T_c value corresponds to $V_{sp}=0.5$. Inset: the T_c vs. B dependence.

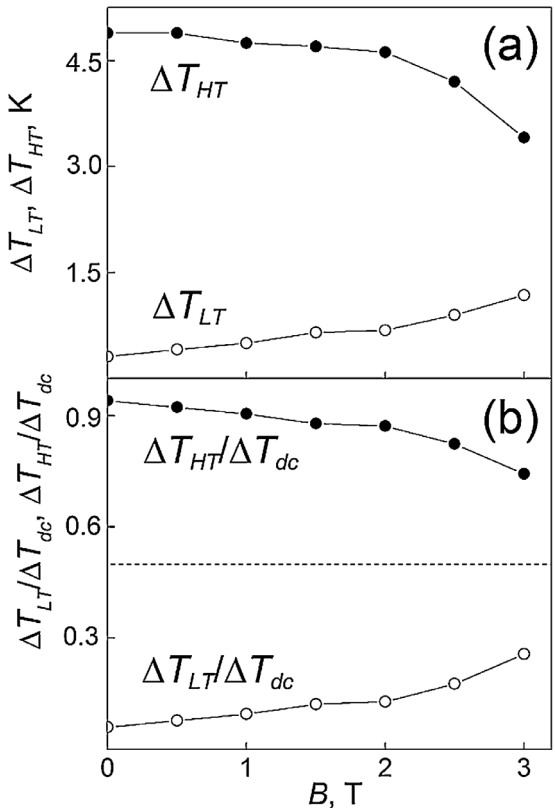

Fig. 7. (a) The magnetic field dependences of the $\Delta T_{HT}= T_d - T_c$ and $\Delta T_{LT}= T_c - T_{c0}$ intervals; (b) The magnetic field dependences of the asymmetry $\Delta T_{HT}/\Delta T_{dc}$ and $\Delta T_{CT}/\Delta T_{dc}$ coefficients.

whereas the $\Delta T_{LT}/\Delta T_{dc}$ values is less 0.5, but at increasing B both asymmetry coefficients gradually tend to 0.5, that is the superconducting transition becomes really more symmetric one under external magnetic field. In other words, magnetic field reduces high-temperature side (above T_c) of the superconducting transition and, at the same time, broads its low-temperature side (below T_c).

According to Figs. 5–7, the superconducting transition is rather broad. As it was mentioned above, this broadening of superconducting transition can be naturally attributed to fluctuation conductivity. Therefore, the superconducting fluctuations developing near the superconducting transition should be taken into account to analyze the B-effect on forming the superconducting state in the nanocomposite. Generally, the corrections to the conductivity due to the superconducting fluctuations, $\delta\sigma$, can be expressed as [1]

$$\delta\sigma = \delta\sigma_{DOS} + \delta\sigma_{AL} + \delta\sigma_{MT}, \tag{7}$$

where $\delta\sigma_{DOS}$ is the correction to the conductivity due to the reduction in the density of states owing to the formation of the virtual

Cooper pairs (DOS), and $\delta\sigma_{AL}$ and $\delta\sigma_{MT}$ are the Aslamazov-Larkin (AL) and Maki-Thompson (MT) contributions to the conductivity.

The AL contribution is related to a forming the non-equilibrium Cooper pairs above temperature of the superconducting transition, resulting in a new contribution to charge transfer. The MT contribution is due to the coherent scattering of electrons (forming the Cooper pairs) on impurities. Near the superconducting transition temperature, but at $T > T_c$, the AL correction is happening to be more important than both the MT and DOS corrections. Then, this contribution can be expressed as

$$\delta\sigma_{AL} \sim \left(\frac{T_c}{T - T_c}\right)^{\beta}, \tag{8}$$

where β is the exponent depending on a dimensionality of the superconducting system (β = 1/2, 1 and 3/2 for the three-dimensional (3D), two-dimensional (2D) and for quasi-one-dimensional (lD) systems, respectively).

In contrast, for low temperatures (at $T << T_c$) the DOS correction becomes important enough. This correction remains finite in the $T \to 0$ limit, i.e. the virtual Cooper pairs are existing even at $T = 0$. Unlike the DOS correction the AL and MT contributions at low temperatures are proportional to T^2 and are gradually vanishing in the $T \to 0$ limit. The temperature dependences of $\delta\sigma_{DOS}$, $\delta\sigma_{AL}$ and $\delta\sigma_{MT}$ at $T < T_c$ are rather complicated. Therefore, let us estimate the AL contribution correction to the conductivity of the nanocomposite only at $T > T_c$. Since $\delta\sigma$ is regarded as excess conductivity, attributed to partially induced superconductive regions in a system above the superconducting temperature transition, $\delta\sigma(T)$ can be determined as

$$\delta\sigma(T) = \sigma(T) - \sigma_n(T), \tag{9}$$

where $\sigma(T)$ is the measured conductivity and $\sigma_n(T) = [\rho_n(T)]^{-1}$ is the normal-state conductivity.

To extract the $\delta\sigma(T)$ dependences, the data presented in Fig. 4 have been used. In this case, $\sigma(T) \sim 1/R(T)$, where the $R(T)$ dependences are the experimental curves, and $\sigma_n(T) \sim 1/R_b(T)$, where the $R_b(T)$ dependences are the fitting lines, corresponding to the hopping conductivity mechanism, which describes the experimental $R(T)$ dependences above the T_d temperature. The normalized fluctuation conductivity, $\delta\sigma(T)/\sigma_d$, have been finally used as

$$\frac{\delta\sigma(T)}{\sigma_d} = [R^{-1}(T) - R_b^{-1}(T)\,]R_d, \tag{10}$$

where $\sigma_d \sim 1/R_d$ is the conductivity at T_d.

The $\ln(\delta\sigma(T)/\sigma_d$ vs. $\ln(\varepsilon)$ dependences taken for different magnetic fields are plotted in Fig. 8. Here, $\varepsilon = (T\text{-}T_c)/T_c$ is the reduced temperature and the maximum T value is limited by T_d. First of all, it is important to note that all of the dependences very well coincide to each other. In other words, the $\delta\sigma(T)/\sigma_d$ vs. ε dependences, taken at different B, form the master curve in the $\ln(\delta\sigma(T)/\sigma_d$ - $\ln(\varepsilon)$ plot, i.e. scaling phenomenon takes place. Next, linear segment indicated by dashed line can be found in Fig. 8.

In accordance with expression (7), the slope of this line allows estimating β. This exponent is equal to ~ 1/2. So, within temperature range corresponding to the linear $\delta\sigma(T)/\sigma_d$ change, the fluctuation conductivity is mainly determined by the 3D AL contribution. Since the temperature $\Delta T_{HT=}\ T_d$ - T_c interval decreases gradually with increasing B (Fig. 7(a)), this contribution is also suppressed under external magnetic field due to destroying the Cooper pairs. It is interesting to note that, in contrast to the $\delta\sigma(T)/\sigma_d$ suppressing under magnetic field at $T > T_c$, this magnetic field at the same time seems to strength the fluctuation conductivity at $T < T_c$, since the $\Delta T_{LT=}\ T_c$ - T_{c0} interval increases gradually with increasing B (Fig. 7(a)). The fluctuation conductivity mechanism should be correctly identified to analyze the B-effect on formation of superconducting state in the PG7 + In nanocomposite.

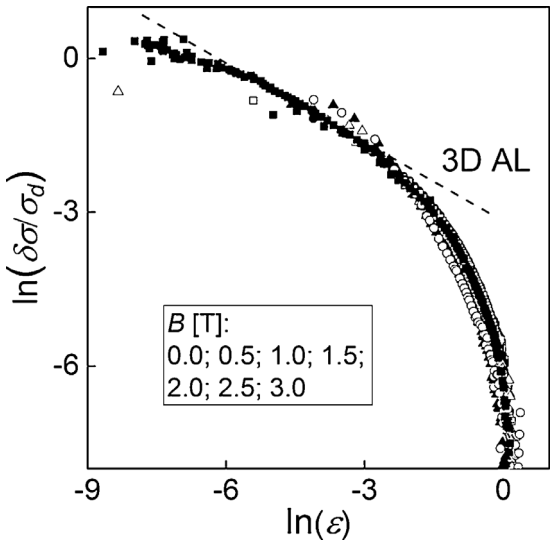

Fig. 8. The $\ln(\delta\sigma)$ vs. $\ln(\varepsilon)$ dependences at various magnetic fields. Dashed line corresponds to the 3D AL contribution.

4. Conclusion

Thus, the superconducting transition has been observed in the nanocomposite PG7 + In. The regularities of the influence of the applied magnetic field on the features of electrical resistance are found and analysed. It is shown that at application of magnetic field the superconducting transition shifts to the lower temperatures. The insulating behavior electrical resistance in a normal state has been satisfactory described in frames of the hopping conductivity mechanism developed for the granular conductor systems. The superconducting transition has been found to be rather broad. This broadening can be explained by the fluctuation conductivity. At temperatures above the superconducting transition the Aslamazov-Larkin contribution to the conductivity has been distinguished.

Declaration of Competing Interest

The authors declare that they have no known competing financial interests or personal relationships that could have appeared to influence the work reported in this paper.

Acknowledgments

A.V. Fokin thanks the Russian Foundation for Basic Researches (grant number 19-02-00760) for financial support of these studies. All of studies were carried out by the scientific equipment of joint research center “Technologies and Materials” at the Belgorod State University.

References

[1] I.S. Beloborodov, A.V. Lopatin, V.M. Vinokur, K.B. Efetov, Granular electronic systems, Rev. Mod. Phys 79 (2) (2007) 469–518, https://doi.org/10.1103/RevModPhys.79.469.
[2] A. Gerber, G. Milner, M.K. Deutscher, A. Gladkikh, Insulator-superconductor transition in 3D granular Al-Ge films, Phys. Rev. Lett 78 (1997) 4277–4280, https://doi.org/10.1103/PhysRevLett.78.4277.
[3] B.A. Abeles, P. Sheng, M.G. Coutts, Y. Arie, Structural and electrical properties of granular metal films, Adv. Phys 24 (1975) 407–461, https://doi.org/10.1080/00018737500101431.
[4] X. Lin, H.M. Jaeger, C. Sorensen, K. Klabunde, Formation of long-range-ordered nanocrystal superlattices on silicon nitride substrates J, Phys. Chem. B. 105 (2001) 3353–3357, https://doi.org/10.1021/jp0102062.
[5] R. Parthasarathy, X.-.M. Lin, K. Elteto, T.F. Rosenbaum, H.M. Jaeger, Percolating through networks of random thresholds: finite temperature electron tunneling in metal nanocrystal arrays, Phys. Rev. Lett 92 (2004) 076801–1-4, , https://doi.org/10.1103/PhysRevLett.92.076801.
[6] D.J. Mowbray, M.S. Skolnick, New physics and devices based on self-assembled semiconductor quantum dots, J. Phys. D. Appl. Phys. 38 (2005) 2059–2076, https://doi.org/10.1088/0022-3727/38/13/002.
[7] J.S. Kim, M. Granström, R. Friend, N. Johansson, W. Salaneck, R. Daik, W. Feast, F. Cacialli, Indium–tin oxide treatments for single- and double-layer polymeric light-emitting diodes: the relation between the anode physical, chemical, and morphological properties and the device performance, J. Appl. Phys. 84 (1998) 6859–6870, https://doi.org/10.1063/1.368981.
[8] A. Fokin, Yu. Kumzerov, E. Koroleva, A. Naberezhnov, O. Smirnov, M. Tovar, S. Vakhrushev, M. Glazman, Ferroelectric phase transitions in sodium nitrite nanocomposites, J. Electroceram 22 (2009) 270–275, https://doi.org/10.1007/s10832-008-9431-4.
[9] I.V. Golosovskya, I. Mirebeau, F. Fauth, D.A. Kurdyukov, Yu.A. Kumzerov, Magnetic structure of hematite nanostructured in a porous glass, Sol. Stat. Commun. 141 (2007) 178–182, https://doi.org/10.1016/j.ssc.2006.10.028.
[10] B.F. Borisov, A.V. Gartvik, E.V. Charnaya, Yu.A. Kumzerov, The effect of melting and crystallization of indium within pores on properties of photonic crystals at different pore fillings, Acoustical Phys 55 (2009) 816–820, https://doi.org/10.1134/S1063771009060165.
[11] Yu.A. Kumzerov, A.A. Naberezhnov, Effect of restricted geometry on the superconducting properties of low-melting metals, Low. Temp. Phys 42 (2016) 1028–1040, https://doi.org/10.1063/1.4971168.
[12] D.K. Finnemore, D.E. Maporther, Superconducting properties of tin, indium, and mercury below 1° K. Phys. Rev. 140 (1965) A507–A518, https://doi.org/10.1103/PhysRev.140.A507.
[13] M.J. Graf, T.E. Huber, C.A. Huber, Superconducting properties of indium in the restricted geometry of porous Vycor glass, Phys. Rev. B 45 (1992) 3133–3136, https://doi.org/10.1103/PhysRevB.45.3133.
[14] J.H.P. Watson, Critical magnetic field and transition temperature of synthetic high-field superconductors, Phys. Rev 148 (1966) 223–230, https://doi.org/10.1103/PhysRev.148.223.
[15] C. Tien, C.S. Wur, K.J. Lin, E.V. Charnaya, Yu.A. Kumzerov, Double-step resistive superconducting transitions of indium and gallium in porous glass, Phys. Rev. B 61 (2000) 14833–14838, https://doi.org/10.1103/PhysRevB.61.14833.
[16] N.K. Hindley, J.H.P. Watson, Superconducting metals in porous glass as granular superconductors, Phys. Rev 183 (1969) 525–528, https://doi.org/10.1103/PhysRev.183.525.
[17] R. Fogclholm, O. Rapp, G. Qrimvall, Electrical resistivity of indium: deviation from linearity at high temperatures, Phys. Rev. B 23 (1981) 3845–3851, https://doi.org/10.1103/PhysRevB.23.3845.
[18] R.W. Simon, B.J. Dalrymple, D. Van Vechten, W.W. Fuller, S.A. Wolf, Transport measurements in granular niobium nitride cermet films, Phys. Rev. B 36 (1987) 1962–1969, https://doi.org/10.1103/PhysRevB.36.1962.
[19] A. Gerber, Low-temperature transport properties of granular Pb films below the percolation threshold, J. Phys. 2 (1990) 8161–8172, https://doi.org/10.1088/0953-8984/2/41/004.
[20] Y. Ando, G.S. Boebinger, A. Passner, T. Kimura, K. Kishio, Logarithmic divergence of both in-plane and out-of-plane normal-state resistivities of superconducting $La_{2-x}Sr_xCuO_4$ in the zero-temperature limit, Phys. Rev. Lett. 75 (1995) 4662–4665, https://doi.org/10.1103/PhysRevLett.75.4662.
[21] T. Abraham, C. Bansal, Logarithmic temperature dependence of conductivity in a random quasi-two dimensional assembly of gold nanoclusters, J. Phys. Commun. 1 (2017) 015008–1-7, , https://doi.org/10.1088/2399-6528/aa81b6.
[22] S. Matsuo, H. Sugiuro, S. Noguchi, Superconducting transition temperature of aluminum, indium, and lead fine particles, Low. Temp. Phys 15 (1973) 481–490, https://doi.org/10.1007/BF00654622.
[23] L.I. Berger, B.W. Roberts, Properties of Superconductors, CRC Handbook of Chemistry and Physics, 90th ed., FL CRC Press, Boca Raton, FlUSA, 2010.
[24] Y. Deguchi, H. Kikuchi, N. Mori, Y. Yamada, T. Atsumi, K. Yoshida, T. Ishibashi, Fluctuation-conductivity characterization of superconducting $Bi_2Sr_2CaCu_2O_{8+d}$ thin films prepared by the metal-organic decomposition method, Phys. Proc. 45 (2013) 193–196, https://doi.org/10.1016/j.phpro.2013.04.086.
[25] A.I. Larkin, A.A. Varlamov, Fluctuation Phenomena in Superconductors, "Handbook on Superconductivity: conventional and Unconventional Superconductors", edited byK.-H. Bennemann and J. B. Ketterson, Berlin, Germany: Springer; 2002.

[26] Yu.A. Kumzerov, A.V. Fokin, L.S. Parfen'eva, B.I. Smirnov, I.A. Smirnov, H. Misiore, A. Jezowski, Thermal conductivity and electrical resistivity of bulk indium and indium embedded in 7-nm channels of porous borosilicate glass, Phys. Solid State 55 (2013) 1779–1785, https://doi.org/10.1134/S1063783413090205.
[27] A.A. Naberezhnov, A.E. Sovestnov, A.V. Fokin, Crystal structure of indium and lead under confined geometry conditions, Techn. Phys. 56 (2011) 637–641, https://doi.org/10.1134/S1063784211050240.
[28] B. Abeles, Effect of charging energy on superconductivity in granular metal films, Phys. Rev. B 15 (1977) 2828–2829, https://doi.org/10.1103/PhysRevB.15.2828.
[29] P.W. Anderson, Lectures on the Mony-Body Problems, Academic, New York, USA, 1964.
[30] Y. Shapira, G. Deutscher, Semiconductor-superconductor transition in granular Al-Ge, Phys. Rev. B 27 (1983) 4463–4466, https://doi.org/10.1103/PhysRevB.27.4463.
[31] M. Gazda, B. Kusz, J. Gackowska, W. Sadowski, Conductivity and superconductivity in granular materials, Acta Phys. Pol. A 114 (2008) 143–148, https://doi.org/10.12693/APhysPolA.114.143.
[32] B.I. Shklovskii and A.L. Efros, Electronic Properties of Doped Semiconductor, Berlin, Germany: Springer; 1984.
[33] O. Ivanov, M. Yaprintsev, Variable-range hopping conductivity in Lu-doped Bi_2Te_3, Sol. St. Sci 76 (2018) 111–117, https://doi.org/10.1016/j.solidstatesciences.2017.12.012.
[34] R. Laiho, A.V. Lashkul, K.G. Lisunov, E. Lahderanta, M.A. Shakhov, V.S. Zakhvalinskii, Hopping conductivity of Ni-doped p-CdSb, J. Phys.: Condens. Mater. 20 (2008) 295204–1-8, , https://doi.org/10.1088/0953-8984/20/29/295204.
[35] R. Laiho, K.G. Lisunov, E. Lahderanta, P.A. Petrenko, J. Salminen, M.A. Shakhov, M.O. Safontchik, V.S. Stamov, M.V. Shybnikov, V.S. Zakhvalinskii, Variable-range hopping conductivity in $La_{1-x}Ca_xMn_{1-y}Fe_yO_3$: evidence of a complex gap in density of states near the Fermi level, J. Phys.: Condens. Mater. 14 (2002) 8043–8055 PII: S0953-8984(02)36797-3.
[36] E. Arushanov, S. Siebentritt, T. Schedel-Niedrg, M. Ch. Lux-Steiner, Hopping conductivity in *p*-$CuGaSe_2$ films, J. Appl. Phys. 100 (2016) 063715–1-4, , https://doi.org/10.1063/1.2338600.
[37] Y.B. Li, Y.Q. Zhang, W.F. Li, D. Li, J. Li, Z.D. Zhang, Spin-glass-like behavior and electrical transport properties of $Cr_7(Se_{1-x}Te_x)_8$, Phys. Rev. B. 73 (2006) 212403–1-4, , https://doi.org/10.1103/PhysRevB.73.212403.
[38] O. Ivanov, O. Maradudina, R. Lyubushkin, Preparation and characterization of bulk composite constructed of Bi_2Te_3@SiO_2 nanoparticles, J. Alloys Compd 586 (2014) 679–682, https://doi.org/10.1016/j.jallcom.2013.10.090.
[39] O. Ivanov, M. Yaprintsev, E. Danshina, Electric field effect on variable-range hopping conductivity in $Bi_{1.9}Lu_{0.1}Te_3$, Phys. B: Condens. Matter 545 (2018) 222–227, https://doi.org/10.1016/j.physb.2018.06.021.